Density Functional Calculations on Actinide Compounds: Survey of Recent Progress and Application to $[UO_2X_4]^{2-}$ (X = F, Cl, OH) and AnF_6 (An = U, Np, Pu)

GEORG SCHRECKENBACH, P. JEFFREY HAY, RICHARD L. MARTIN

Theoretical Division (MS B268) and Seaborg Institute for Transactinium Science, Los Alamos National Laboratory, Los Alamos, New Mexico 87545

Received 12 June 1998; accepted 20 August 1998

ABSTRACT: The subject of this article, the application of density functional theory (DFT) to molecular systems containing actinide elements, is discussed in two parts. In the first part, a survey is given of DFT applications on actinide-containing molecules. Various methodological developments are reviewed, including, among others, new relativistic effective core potentials (ECP), and newly developed stable relativistic DFT methods. Actual DFT calculations of actinide molecular systems are discussed, covering the time from about 1991 to the present. In the second part, two different DFT-based relativistic methods are applied to some actinide molecules. These are ECPs and the quasirelativistic (QR) method. Systems studied include actinide hexafluorides AnF_6 (An = U, Np, Pu) and uranyl (VI) anions $[UO_2X_4]^{2-}$ (X = OH, F, Cl). Calculated geometries and vibrational frequencies are discussed and compared with experiment. The two relativistic methods have been combined with the BLYP and B3LYP density functionals. The ECP-B3LYP and QR-BLYP approaches gave the best bond lengths and frequencies. The existence of stable structures with a bent uranyl bond (''cis-uranyl'') is predicted for all three $[UO_2X_4]^{2-}$ ions. ECP-B3LYP predicts the following order for the stability of the ''cis'' conformers of $[UO_2X_4]^{2-}$ (relative to the respective global energy minimum): OH > F > Cl

Correspondence to: J. Hay

Contract/grant sponsors: Laboratory Directed Research and Development Program of the Los Alamos National Laboratory; U.S. Department of Energy; Seaborg Institute for Transactinium Science

CCC 0192-8651 / 99 / 010070-21

with the ''cis''-$[UO_2Cl_4]^{2-}$ being least stable. The article concludes with a discussion of future directions for the application of DFT to the f-block chemistry.
 J Comput Chem 20: 70–90, 1999

Keywords: density functional theory; actinide compounds; relativity; uranyl complexes; effective core potentials

Introduction

The chemistry of the actinide elements is an important research area for quantum chemistry. Fundamental interest arises because f-type atomic orbitals can participate in the chemistry of these elements, leading to interesting new bonding schemes as compared with the transition metals or main group elements. The radioactivity of actinide atoms presents a strong practical motivation for theoretical studies to provide useful data on actinide molecular processes where experimental probes may be difficult to apply.

A 1991 review article by Pepper and Bursten[1] described the theoretical investigation of actinide chemistry as ''a challenge to applied quantum chemistry.'' Today, the challenge remains, in spite of considerable progress over the last 8 years; that is, actinide chemistry is still far from being a routine area for the application of quantum chemistry. There are several problems that have to be solved in one way or another. First, the actinide elements comprise the heaviest part of the periodic table. Consequently, there are very many electrons that have to be dealt with, most of them occupying inert core shells. Second, scalar and often also spin–orbit relativistic effects have to be included for even a qualitative understanding of the f-block chemistry. Third, correlation effects resulting from the interaction between the electrons are at least equally important. Finally, the 5f, 6d, 7s, and 6p orbitals are comparatively close in energy and spatial extent and can all participate in bonding. This is illustrated in Figure 1 where the radial probability densities are plotted for the valence orbitals of Pu.[2,3] In addition, for the 5f orbitals there are

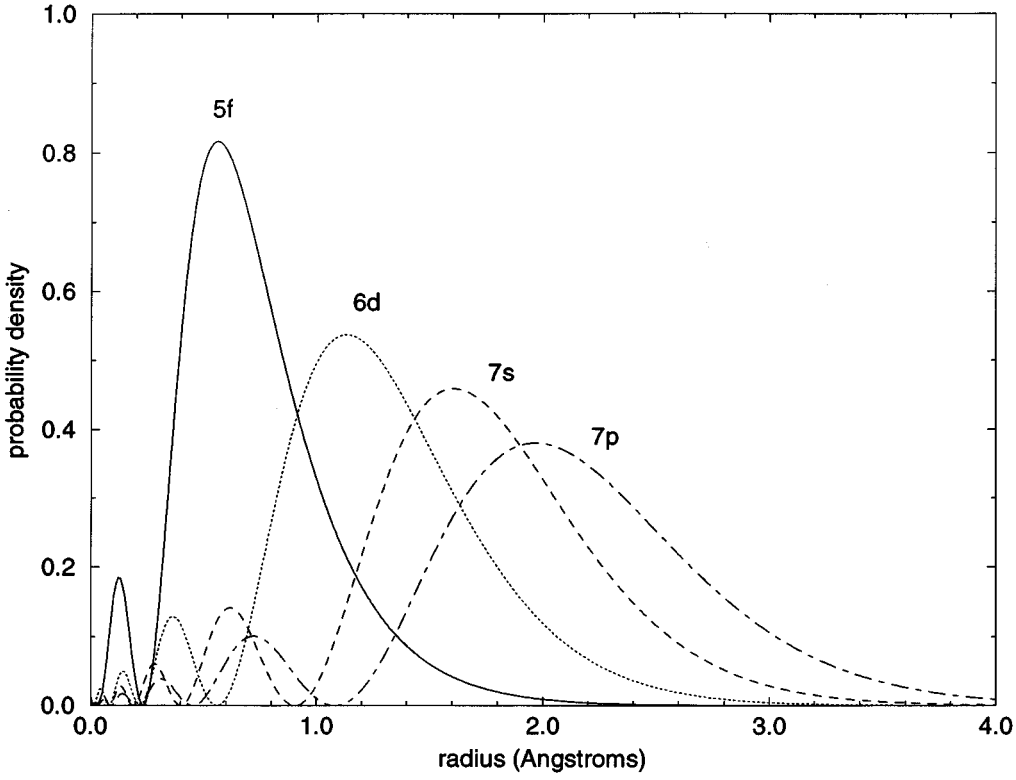

FIGURE 1. Radial probability densities of Pu valence orbitals from relativistic atomic calculations (see text and ref. 2).

typically degeneracies or near degeneracies present in a molecule, which makes it difficult to achieve convergence in the self-consistent solution of the quantum-mechanical equations or to describe excited states.

In this article, we examine the state of affairs regarding the application of density functional theory (DFT)[4–12] to actinide compounds. Much progress has been achieved in the quantum chemistry of the actinides since the mentioned 1991 review.[1] A major part of these advancements has been accomplished with DFT-based methods, and we will review the respective literature in the following section, the first part of the article. DFT is particularly attractive because it includes electron correlation in a very efficient manner. Additionally, scalar and spin–orbit relativistic effects can be included in a relatively straightforward manner. What can and cannot be done today is illustrated in the second part of the article where we present results for f^0 uranyl (VI) compounds, $[UO_2X_4]^{2-}$, X = F, Cl, and OH, as well as for hexafluorides, AnF_6, An = U, Np, and Pu (formally f^0, f^1, and f^2, respectively). We use these series to compare two well-established relativistic approaches that are in wide use: relativistic effective core potentials (ECP)[13–15] and the quasirelativistic (QR) method[16–20] that employs a Pauli Hamiltonian.[21–26] We will compare calculated ground-state geometries and vibrational frequencies between these two methods and, where possible, with experiment. Finally, an outlook on possible future directions will conclude the article.

Overview of Relativistic Density Functional Calculations on Actinide Complexes

RECENT REVIEW COVERING RELATIVISTIC EFFECTS AND ACTINIDE TOPICS

The importance of relativity for chemical phenomena is now widely recognized, and numerous reviews are available. Relativistic effects can be defined as anything arising from the finite speed of light, $c = 137.03599$ in atomic units (a.u.),[27] as compared with a hypothetical infinite value for this natural constant. The 1988 review by Pyykkö[28] is perhaps the classic reference on relativistic effects in chemistry.

Pepper and Bursten[1] have given a detailed and thorough review of theoretical calculations on actinide molecules, and we can refer to this article for studies up to about 1990–1991. They have also discussed the theoretical methods that were available at the time. Older reviews have been summarized (e.g., by Pyykkö[29] and by Hess[30]). Recent reviews on actinide topics include a discussion of theoretical and experimental work on the electronic structure and bonding in actinyl ions,[31] a discussion of bonding in cyclopentadienyl–actinide complexes by Bursten and Strittmatter,[32] and a similar article covering lanthanocenes and actinocenes by Dolg and Fulde.[33] Several more general reviews on relativistic effects were also published. Electronic structure calculations on transactinides and their compounds were reviewed by Pershina[34] in an article that contains a detailed summary of various relativistic methods. Almlöf and Gropen[35] presented a fairly mathematical introduction to relativistic quantum mechanics and to relativistic effects in chemistry. Kaltsoyannis[36] focused on qualitative aspects of relativity and chemical bonding, including a section on the organometallic chemistry of f-elements. Two reviews were published by Hess et al.[30,37] Both contain theory and applications; one of them[37] focuses on spin–orbit effects, whereas the other[30] emphasizes scalar relativistic effects and the importance of electron correlation. Engel and Dreizler[38] have reviewed the theoretical foundations of relativistic DFT. King published an article[39] that discusses actinide bonding based on group theory and the topological properties of f-orbitals. Dolg presented a short review[40] that covers, in a concise manner, various aspects related to theoretical studies on lathanides and actinides. Finally, two other recent reviews focus mostly (Balasubramanian[41]) and exclusively (Dolg[42]), respectively, on lanthanide-containing molecules. Both reviews discuss relativistic methods, and the review by Balasubramanian[41] has a short section on actinide molecules as well.

METHODOLOGICAL ASPECTS

Methodological aspects have been developed considerably during the last decade. New approaches have been proposed for the approximate description of relativistic effects, for an accurate description of electron correlation, and for the determination of various properties of the heavy elements and their compounds. All of these developments have already made a strong impact on theoretical actinide chemistry or will do so in the near future. We will discuss some of the achievements in these three areas next.

Relativistic methods. To start with the quantum-mechanical description of relativistic effects, first-principle relativistic methods can be roughly divided into four-component methods that are based directly on the full Dirac[43,44] (or Dirac–Breit[45]) equation, and into more approximate but computationally less demanding two- or one-component approaches. A new four-component program package, the Beijing density functional package (BDF) has recently been presented.[46,47] This program is a significant improvement over older DFT-based four-component methods,[48–51] in particular because it allows the use of accurate models for the exchange-correlation (XC) functional of DFT.

Two- or one-component methods can be divided further into schemes that approximately decouple the ''large'' and ''small'' components[24–26] of the Dirac equation by means of some appropriate transformation and methods that employ relativistic effective core potentials (ECP). Two new approaches have been proposed which overcome well-known difficulties[52] of the Pauli operator.[21–24]. Rösch and coworkers implemented the Douglas–Kroll (DK) method[53–55] within a DFT framework.[56–59] The proper use of the DK transformation within the DFT framework has subsequently been debated.[60,61] Boettger[62] has used the DK Hamiltonian to study certain approximations made by Rösch et al., and finds them to be valid as long as spin–orbit splitting is not important. His test systems included the plutonium atom, among others. Baerends and van Lenthe developed the ''zero-order regular approximation'' (ZORA) to relativistic effects, again in the framework of modern DFT.[63–66] Neither the DFT-ZORA method nor the DFT-DK approach has yet been applied to actinide chemistry, although such projects can be expected soon. Both methods have given comparable results for a few nonactinide test cases.[67] Dyall[68] has developed a new approximate relativistic method that is based on the well-known ''elimination of the small component'' method.[24,25] Dyall's approach uses relativistic metrics throughout, and avoids the shortcomings of the Pauli Hamiltonian,[21] but has not been extended to DFT. Applications to triatomic actinide molcules have been carried out.[69]

Relativistic ECPs are arguably the most widely used relativistic method for practical chemical applications. In ECP schemes,[14,15] the chemically inert core electrons are replaced by an effective potential. This results in substantial savings of computational resources as it reduces the number of electrons in the system dramatically. The major relativistic effects are included if this potential had been derived from fully relativistic atomic calculations. New nonrelativistic[70] and relativistic ECPs[13,70–72] for the actinide elements have been published, along with the appropriate basis sets. In some cases, the corresponding spin–orbit operators have also been proposed.[70–72] The transferability of *ab initio* (Hartree–Fock)-derived ECPs into DFT studies has been discussed.[73,74] No major problems have been found, although test cases do not yet include actinide molecules.

Correlation. Hess, in his recent review,[30] points out that the accurate treatment of electron correlation effects is much more demanding than the inclusion of relativity. For the treatment of correlation effects, there are two principal avenues. These are *ab initio* and DFT methods, and the methods are, in most cases, the same in nonrelativistic and relativistic calculations. Considerable progress has been achieved in both areas, and the theoretical description of the actinide chemistry has benefited from them. Available (nonrelativistic) correlated *ab initio* methods have been reviewed (e.g., by Raghavachari and coworkers[75,76]; by Bartlett[77]; and, from a very general point of view, by Head-Gordon[78]).

DFT includes electron correlation implicitly and efficiently,[12] but the difficulty is in finding accurate approximations for the (unknown) exchange-correlation (XC) functional.[6] Older calculations, including those reviewed by Pepper and Bursten[1] used the simple local density approximation (LDA),[79] often in its even simpler X-alpha version.[80] Typically, the LDA is insufficient to yield correct bond energies or metal–ligand bond distances.[7,8] Post-LDA methods, including generalized gradient approximations (GGA)[81–84] and hybrid functionals[85–87] have become generally available in the last few years. As a result, the accuracy of DFT energies are now often comparable with traditional correlated *ab initio* methods. At the same time, the computational cost is much smaller than for highly correlated *ab initio* methods, and DFT is frequently the only practical choice for larger transition metal systems. Likewise, theoretical actinide chemistry has benefited from these advances in DFT. Indeed, much of the study on actinide complexes is now done within the density functional framework (see later).

There is at least one subtle point in the application of relativistic DFT.[38] Namely, the exact, unknown XC functional will not be the same for the nonrelativistic and relativistic formulations.[38] In-

deed, approximate relativistic functionals have been proposed.[88–90] Such functionals, along with the effects of a finite nucleus, have recently been tested by Mayer et al.[67] on gold diatomics. The tests have been performed in the framework of the DK approximation. Mayer et al. found that neither relativistic corrections to the XC functional nor effects of a finite nucleus affect calculated molecular properties in any appreciable way—a rather reassuring result!

Properties. Equally important for the accurate description of the electronic structure is the subsequent calculation of various molecular properties that allow direct comparison to experiment. The single most important property is the equilibrium geometry of the molecule. This requires geometry optimizations.[91] They rely on the calculation of the forces at any given geometry, using first derivatives of the total energy with respect to nuclear coordinates, and possibly second derivatives. Second derivatives allow, in turn, the determination of force constants and vibrational frequencies.[91] Significant progress has been achieved for DFT methods that are applicable to molecules with heavy atoms. Schreckenbach et al. presented the implementation of analytical forces for the DFT-QR method,[92,93] thus enabling automatic optimizations of molecular structures including relativistic effects. Nasluzow and Rösch achieved the same for the DFT-DK approach.[59] In the ECP field, Breidung et al.,[94,95] Russo et al.,[96] and Ciu et al.[97] implemented analytic second derivatives. They allow the routine calculation of vibrational frequencies and can also be used to support geometry optimizations in difficult cases.

Another important property is the NMR chemical shift. Although calculations on actinide-containing molecules have not been reported to date, the theoretical means have become available recently. Kaupp et al.[98,99] have presented the calculation of NMR chemical shifts based on DFT and the use of ECPs. The chemical shift of light nuclei can be calculated, including scalar relativistic effects, if a relativistic ECP is used on the heavy atom(s) in the system. Malkin et al.[100] presented a method for the calculation of spin–orbit corrections to the NMR chemical shift. Spin–orbit can, at times, be the major relativistic effect on the chemical shift. Schreckenbach and Ziegler[93,101,102] have extended the DFT-QR method to the NMR chemical shift. Thus, scalar relativistic effects on the chemical shift of both heavy and neighboring light atoms became accessible.[102,103] Wolff and Ziegler[104] have extended this approach to include spin–orbit effects as well. Recently, they have also used the more accurate DFT-ZORA approach for the NMR chemical shift.[105] All of those methods are available for actinide-containing molecules; none has yet been applied, although work is in progress.[106] DFT calculations of NMR chemical shifts have recently been reviewed[107] with special emphasis on relativistic effects—reliable relativistic calculations of NMR chemical shifts are so far only possible with DFT-based methods.

THEORETICAL CALCULATIONS ON ACTINIDE-CONTAINING MOLECULES

A variety of theoretical approximations have been applied to actinide problems. In what follows, we concentrate mostly on DFT-based methods, in agreement with the scope and purpose of this article. We should point out that *ab initio*-based methods[108] have been applied to actinide molecules as well.[33,109–133]

The older ''discrete variational X-alpha'' (DV-X_α) approach of Ellis and coworkers[48–51] is still very popular; it is an effective, fully relativistic, DFT-based four-component method. As the acronym suggests, the simple X_α approximation[6,80] is used for the XC functional. This will prevent quantitative agreement of calculated energetics or bond lengths with experiment. Nevertheless, a detailed understanding of excited states, relativistic effects, or of the molecular orbitals and electronic structure is possible. The DV-X_α method has been applied to a number of different actinide molecules. Problems studied include the photoelectron spectrum of actinide tetrahalides AnX_4 (An = U, Th; X = F, Cl),[134] the photoelectron spectrum and electronic structure of cyclopentadienyl complexes $U(\eta^5\text{-}C_5H_5)_3L$ (L = —CH_3, —NH_2, —BH_4, —NCS)[135] and $(\eta^5\text{-}C_5H_5)_3MOCH_3$ (M = Ce, Th, U),[136] and of tetravalent thorium metallacyclobutane metallocene complexes,[109,137] the electronic structure and ionization energies of pentavalent uranium imide and amide complexes,[138] a comparison among metal carbonyls $M(CO)_6$ (M = Cr, W, U, Sg),[139] the electronic structures and optical transition energies of NpF_6, UX_6^{1-} (X = F, Cl, Br), PaX_6^{2-} (X = F, Cl, Br, I)[140] and $Th(\eta^5\text{–}C_5H_5)_3$ and $Pa(\eta^5\text{-}C_5H_5)_2$,[141] the electronic structure, bonding, relativistic effects,[142–144] and UV excited states[145] of UF_6, the bonding in AnF_6 (An = U, Np, Pu),[144] and a comparison between C_{4v} and D_{3h} geometries of monomeric UF_5.[146] All of those calculations were done at fixed geometries only. The simpler ''X_α-scattered wave'' technique[3,147] (that applies a

''muffin-tin'' approximation for the atomic potential) has been applied to single-point calculations on conformers of the model compounds U_2H_{10} and $U_2(OH)_{10}$[148] as well as to the study of bonding and periodic trends in $An(\eta^5\text{-}C_5H_5)_3$ complexes (An = U, Np, Pu, Am, Cm, Bk, Cf, and lanthanides).[149] *ab initio*-based four-component methods have also been applied to small actinide-containing molecules.[115–119]

Two- and one-component relativistic methods have been used in other recent applications. Such methods are less rigorous than four-component approaches in their treatment of relativistic effects. They allow one, however, to use more accurate versions of DFT (i.e., GGA[81–84] or hybrid functionals[85–87]) or to calculate equilibrium geometries and vibrational frequencies. Van Wezenbeek et al.[150,151] discussed the relativistic bond lengthening in UO_2 and UO_2^{2+}. They used the DFT-QR method[16–20] and a simple version of DFT (X_α[6,80]) to determine the equilibrium geometries and potential energy surfaces. Haaland et al.[152] used the same DFT-QR method, together with a GGA,[81,82] to find the structure and vibrational frequencies of UCl_4, an f^2 system. This article by Haaland[152] is an interesting example of theory being used to augment experimental work. Another example is given by some recent work of Andrews and coworkers,[153–156] who used the DFT-QR approach to support their gas-phase studies of small molecular clusters. Molecules studied included uranium[153] and thorium[155] hydride species (AnH, AnH_2, AnH_3, AnH_4 for An = U and Th; U_2H_2; and U_2H_4), products of the reaction of laser-ablated uranium with NO, NO_2, and N_2O,[154] and various An_xN_y and An_xO_y clusters (An = Th, U, Pu; x = 1, 2; y = 1–4).[156] In each case, the geometries, electronic structures, and vibrational frequencies were calculated and used to interpret the experimental data. Heinemann and Schwarz[157] applied the DFT-QR method to study the geometry and electronic structure of their newly synthesized NUO^+ ion. This ion is isoelectronic to the well-known uranyl ion UO_2^{2+}, and its existence had been predicted earlier by theoretical methods.[158] Kaltsoyannis[159] applied relativistic DFT (GGAs and X_α), including spin–orbit, to calculate $f \rightarrow f$ transition energies of the f^1 complexes $[PaX_6]^{2-}$ (X = F, Cl, Br, I). A simple scaling of the X_α approach gave better results than the more modern GGAs in these cases. Kaltsoyannis and Scott[160] have also studied the electronic structure of $[\{(NH_2)_3(NH_3)U\}_2(\mu^2\text{-}\eta^2\text{:}\eta^2\text{-}N_2)]$. They used this complex as a model compound for a recently synthesized, much larger, dinitrogen uranium cluster.[161]

Li and Bursten[162] published an extensive study of cycloheptatrienyl sandwich complexes $An(\eta^7\text{-}C_7H_7)_2^q$ (An = Th, Pa, U, Np, Pu, Am; q = 2−, 1−, 0, 1+). They used the DFT-QR method and a GGA[81,82] to calculate and discuss geometries, electronic structure, ionization energies, bond energies, oxidation states, and other properties of these complexes of which $U(\eta^7\text{-}C_7H_7)_2^{1-}$ is currently the only experimentally known example.[163] The fairly uncommon D_{7h} symmetry has been used in these calculations. A rather interesting result is that oxidation or reduction of such complexes should involve primarily ligand-based electrons. In other words, the cycloheptatrienyl ligands act as an ''electron sponge.''

Li and Bursten have further studied[164] the endohedral fullerene complexes of the early actinides $M@C_{28}$ (M = Th, Pa, U, Np, Pu, Am, among others), again using the DFT-QR method, including a GGA.[84] Geometries have been fully optimized. Vibrational frequencies, bonding energies, ionization energies, and electron affinities have been calculated. Scalar relativistic effects only have been included to determine geometries and vibrational frequencies. However, single-point calculations including spin–orbit effects were used to discuss bonding schemes and the electronic structure of these compounds. The actinide metals are in each case located in the center of the fullerene, and they form strong covalent bonds to the cage that shows a large f-orbital involvement. Thus, all the endohedral complexes (which have not yet been isolated experimentally) are predicted to be stable. The C_{28} cages are deformed when a metal is inserted. Two effects are competing: steric and electrostatic effects that tend to expand the cages, and covalent effects that tend to contract them.

Li and Bursten have also explicitly investigated spin-orbit effects as they manifest themselves in the electronic structure, electronic transitions, and ionization energies of protactinocene, $[Pa(\eta^8\text{-}C_8H_8)_2]$,[165] as well as the cycloheptatrienyl anion, $[U(\eta^7\text{-}C_7H_7)_2]^-$.[166] In the protactinocene study,[165] they found that scalar relativistic and spin-orbit calculations result in different ground-state electron configurations [scalar relativistic: $(f\sigma)^1$; spin–orbit: $(f\varphi)^1$, $E_{5/2u}$]. Such spin–orbit calculations require the use of double-group symmetry.

ECPs have been used with DFT. Thus, we have recently studied[167] the structure, stable isomers, vibrational frequencies, and ligand exchange of the newly characterized[168] uranyl (VI) tetrahydroxide

$[UO_2(OH)_4]^{2-}$. The existence of stable structures with a bent uranyl bond (''cis-uranyl'') has been predicted (see later). Furthermore, we have applied[13] ECPs and examined various typess of DFT in actinide hexafluorides, AnF_6 (An = U, Np, Pu). Both species are also discussed later. Actinide ECPs have been used extensively with *ab initio* methods as well.[33,40,109–111,120–133]

Applications

THEORETICAL METHODS

So far, we have reviewed the available DFT methodology as well as recent calculations. We will now turn to more specific applications carried out in our own group. We have investigated two different DFT-based approaches to describe the relativistic effects in actinide-containing molecules, the QR method and relativistic ECPs. Before going into the technical details, it is worthwhile to discuss the differences and common features of the two DFT approaches.

The DFT-QR method has been developed by Snijders, Ziegler, and coworkers.[16–20] An approximate description of the major relativistic effects is achieved by subjecting the fully relativistic, four-component Dirac–Kohn–Sham equations[38] to a series of Foldy–Wouthuysen transformations.[22,23] The result is, in the magnetic-field-free case (with which we are exclusively concerned), a set of two-component equations that resemble the nonrelativistic Kohn–Sham equations but contain, in addition, the so-called mass–velocity, Darwin, and spin-orbit operators. The relativistic operator is known as the Pauli operator.[21–26,28] The contributions to the relativistic Pauli operator are, in this order, given by:

$$h^{MV} = -\frac{1}{8c^2}p^4 \tag{1}$$

$$h^{Dar} = \frac{1}{8c^2}\nabla^2 V \tag{2}$$

and

$$h^{SO} = \frac{1}{4c^2}\vec{\sigma}\cdot\left[\vec{\nabla}V \times \vec{p}\right] \tag{3}$$

where we have used atomic units. Furthermore, c is the speed of light, $\vec{p}$ is the electronic momentum operator, $\vec{\sigma}$ is the electronic spin operator, and V is the total Kohn–Sham potential that arises from the nuclei and the electronic density. It is a good approximation to use only the potential of the nuclei and the core electronic density instead of the full potential V[19]; we will adopt this approximation in the following. The operators of eqs. (1)–(3) have a well-known physical interpretation[23–26]; h^{MV} and h^{Dar} are corrections to the nonrelativistic kinetic and potential energy operators, respectively[63,169], whereas h^{SO} describes the spin–orbit coupling. Neglecting h^{SO} of eq. (3) results in a one-component equation that is called the scalar relativistic approximation. We will use this additional approximation in the following.

The details of the QR method and its implementation into DFT have been given elsewhere.[16–20,92,93] However, we have to mention that the self-consistent use of Pauli-type Hamiltonians has been criticized in the literature. This is because the Pauli operator has been derived from perturbation theory,[52] and it has been argued that it should not, at least in principle, be used beyond first-order perturbation theory. Thus, it is known that the mass–velocity correction to the kinetic energy operator is valid only for small electron velocities.[169] It is wrong if the instantaneous electronic velocities approach the speed of light. In particular, core electrons have a high probability of being close to the nucleus. Therefore, they obtain high instantaneous velocities,[28] and the mass–velocity correction of eq. (1) becomes invalid for heavy nuclei. Furthermore, a Hamiltonian containing this mass–velocity operator has negative eigenvalues.[169] This may lead to a variational collapse—that is, to arbitrarily large negative eigenvalues of the Kohn–Sham equations. Both problems can be circumvented at once in the QR method by using the frozen-core approximation.[18,20,170–172] In the frozen-core approximation, the orbitals describing the highly relativistic core electrons are assumed to be the same in atomic and molecular systems. Hence, those orbitals are computed in atomic calculations, and kept frozen thereafter. In the relativistic case, they are treated with the complete four-component Dirac equation.[23–25,43,44] The core electron density and its potential are extracted from these fully relativistic calculations. They are used in the subsequent molecular calculations. The remaining valence electrons are, on the other hand, far from the core and have small average velocities, so that the QR expressions should be applicable. The variational collapse is further avoided by a proper choice of valence basis functions. The respective requirements have been discussed in more detail by van Lenthe[173]; the basis sets that

are employed here fulfill the requirements, and no variational collapse occurs. The QR method has been employed in practical calculations, with remarkable success (cf., e.g., the actinide examples cited earlier[153–157, 162, 164]).

ECP methods[14, 15] use an approach that is similar to the idea of the frozen-core approximation and the QR method. They, too, aim at excluding the chemically invariant but highly relativistic core electrons from the variational treatment. In typical ECP methods, this is done by using an effective potential that represents the effects of the core electrons. At that point, there is an important difference between the frozen-core and ECP methods. It concerns the core region of the valence orbitals. In the frozen-core approach, valence orbitals are orthogonalized against the core. This ensures, at least approximately, the proper asymptotic behavior near the nucleus. In ECP schemes, however, the valence pseudo-orbitals have, by construction, the wrong asymptotic behavior in the core region, because the ''core wiggles'' are ''smoothed away.'' This ansatz can be advantageous or disadvantageous, depending on the question at hand: the core behavior is irrelevant if pure valence properties, like geometries or bonding energies, are required, and neglecting these ''core wiggles'' eases the requirements on the basis sets. On the other hand, core-type properties (e.g., the metal NMR shielding) cannot easily be calculated with pseudo-orbitals but are accessible to the frozen-core approximation.[101] Another, more minor difference between the QR and ECP schemes concerns the treatment of direct relativistic effects in the valence orbitals: such effects are included explicitly in the QR scheme by using the relativistic operators of eqs. (1)–(3) [or eqs. (1) and (2) in the scalar relativistic case]. They do not appear in ECP schemes, which implicitly include the relativistic effects in the effective potential, although spin-orbit effects can be accounted for.[70–72] Relativistic ECP and QR schemes have given geometries and energetics of comparable quality[174, 175]; this shows that the major relativistic effects have been accounted for by either method.

COMPUTATIONAL DETAILS

Scalar relativistic ECP calculations were done with the Gaussian-94 program package.[176] A locally modified version of Gaussian-94[96] has been employed to obtain analytic first and second derivatives of the total energy with respect to nuclear displacement. Such derivatives are essential to optimize geometries and to calculate vibrational frequencies. The basis sets are the same as in our previous studies[13, 167]: On U, Np, and Pu, general ECP valence basis sets[13] are employed in the [3s3p2d2f]-contracted (AnF_6) or completely uncontracted ($[UO_2X_4]^{2-}$) versions. On the ligand atoms, the standard 6-31G* (F in AnF_6) or 6-31 + G* (O, X in $[UO_2X_4]^{2-}$) all-electron basis sets are used.[177]

We performed scalar relativistic DFT-QR calculations using the Amsterdam Density Functional program package ADF[170–172, 178–181] One important feature of the ADF program is the exclusive use of numerical integration for (almost) all relevant integrals. The accurate numerical integration scheme is the work of te Velde et al.[181–183] Standard uncontracted Slater-type basis sets (STO basis sets)[184–186] were employed. We used the ADF basis IV on actinide elements and V on the light ligands. These are triple-ζ valence basis sets that contain one (U, Np, Pu) or two (ligands) sets of polarization functions. The atomic orbitals up to and including the 5d shell on U, Np, and Pu, the 1s shell on C, O, and F, and the 2p shell on Cl were considered as core and treated by the frozen-core approximation[170] as outlined earlier. A set of auxiliary s, p, d, f, and g STO functions, centered on all nuclei, is part of an ADF standard basis set. It was employed to fit the electron density and to represent the density-dependent Coulomb and XC potentials accurately in each SCF cycle.[186] Analytic first derivatives of the total energy with respect to nuclear displacement are available in ADF and have been used for geometry optimizations. Analytic second derivatives[187, 188] are not yet available, but vibrational frequencies can be calculated with the more costly numerical second derivatives.[189]

Achieving SCF convergence can be a problem in actinide calculations. This is, in fact, more so for DFT calculations than for Hartree–Fock, due to the larger HOMO–LUMO gap in Hartree–Fock theory.[12, 26] In Gaussian calculations, we have used a procedure of ''building the guess,'' as described elsewhere.[167] In the ADF program, use is made of the molecular symmetry, and the program assigns equal fractions of an electron to symmetry degenerate, partially filled valence orbitals—an ansatz that has been beneficial for the SCF convergence.

We used the following exchange-correlation (XC) functionals. As an example for the generalized gradient approximation (GGA), calculations were performed with the Becke exchange functional,[81, 86] combined with the Lee–Yang–Parr correlation functional[83] (BLYP). This functional allows direct comparisons of the different relativistic ap-

proaches, because it is available both in the ADF and in the Gaussian programs—except for differences in the numerical integration schemes and, in particular, in the basis sets including the auxiliary fit basis of ADF. Additionally, calculations were done with the B3LYP hybrid functional. The B3LYP combines the Lee–Yang–Parr correlation part[83] with the three-parameter hybrid exchange functional of Becke[85] that contains part of the ''exact'' Hartree-Fock exchange. The B3LYP functional is currently not available in ADF. Hence, only ECP calculations have been performed with this functional.

Results and Discussion

The hexafluorides of the early actinides are an interesting test case for theoretical methods,[1, 13, 117, 118, 140, 142, 145] particularly because they are exceptionally well characterized by experimental methods.[190–197] We will use them here to test and compare the different theoretical methods, by applying such methods to the bond lengths and vibrational frequencies of AnF_6 molecules,[13] An = U, Np, and Pu. This series provides an example of f^0, f^1, and f^2 systems.

Central to the aqueous chemistry of uranium and other actinide elements are their complexes with water, the hydroxide ion, and other common aqueous ligands such as CO_3^{2-}, F^-, and Cl^-.[198] For the higher valence states, such as U(VI), a prominent role is played by the very stable uranyl UO_2^{2+} ions and their complexes.[31] We have recently studied[167] the uranyl (VI) tetrahydroxide $[UO_2(OH)_4]^{2-}$. This compound has been found in alkaline solutions containing the uranyl ion UO_2^{2+} and has been characterized extensively by Clark et al.[168] One important finding of our investigations[167] was the prediction of stable conformers with a bent uranyl bond (''cis-uranyl''). Such structures are experimentally unknown, but appear to play an important role as short-lived intermediates in oxygen ligand exchange processes. We will, with the present investigations, extend these studies to other ligand systems, including the F^- and Cl^- ligands. Both $[UO_2F_4]^{2-}$ and $[UO_2Cl_4]^{2-}$, have occasionally been studied by theoretical methods.[158, 199, 200] The electronic structure of $[UO_2Cl_4]^{2-}$ was discussed earlier by Pershina et al.,[199, 200] based on the simple scattered-wave technique and an assumed geometry. Pyykkö et al.[158] calculated the geometry of $[UO_2F_4]^{2-}$ using ECPs[201] and Hartree–Fock theory. Vibrational frequencies or the possibility of ''cis-uranyl'' conformers were not discussed in either work.

TABLE I.
Calculated and Experimental Bond Lengths in AnF_6 Molecules (An = U, Np, Pu; O_h Symmetry).

Method	An — F bond length (Å)		
	UF_6	NpF_6	PuF_6
ECP-B3LYP[a]	2.014	2.013	1.985
ECP-BLYP[a]	2.043	2.047	2.019
QR-BLYP	2.010	1.996	1.981
Experimental[b]	1.996(8)	1.981(8)	1.971(10)
Experimental[c]	1.999(3)		

[a] Ref. 13.
[b] Ref. 191.
[c] Ref. 190.

1. HEXAFLUORIDES AnF_6 (An = U, Np, Pu)

Calculated[13] and experimental[190, 191] bond lengths of the hexafluorides are given in Table I. We note that the agreement of theory and experiment is closest for the QR-BLYP and the ECP-B3LYP approaches, whereas QR-BLYP is superior to ECP-B3LYP for NpF_6. The experimentally observed actinide contraction is best reproduced by QR-BLYP. The QR-BLYP and ECP-BLYP calculations both employ the same gradient corrected density functional.[83, 85] Differences arise from the use of uncontracted Slater basis functions and auxiliary density fits in the former case, and contracted Gaussian basis functions in the latter, as has been pointed out before.

The trends in observed bond lengths and calculated vibrational frequencies are shown in Table II. Vibrational frequencies are known to be sensitive to the reference geometry. They can, in principle, be calculated at any given geometry,[202–206] but we performed frequency calculations only at optimized geometries. Upon comparison of calculated and experimental frequencies, the close agreement between the QR-BLYP geometries and experiment leads to an average deviation of only 7 to 8 cm^{-1} in the frequencies. The average deviations for the other two methods are 14, 19, and 30 cm^{-1} for UF_6, NpF_6, and PuF_6 (ECP-B3LYP) and 29, 37, and 33 cm^{-1} (ECP-BLYP), respectively.[13]

One potential error source results from the effects of anharmonicity that are present in experimental vibrational frequencies, but are neglected by the current theoretical approaches. Experimen-

TABLE II.
Calculated (QR-BLYP[a] and ECP-B3LYP[b]) and Experimental[c] Vibrational Frequencies of AnF_6, An = U, Np, Pu (in cm^{-1}).

	UF_6			NpF_6			PuF_6		
Mode	QR-BLYP[a]	ECP-B3LYP[b]	Exp.[c,d]	QR-BLYP[a]	ECP-B3LYP[b]	Exp.[c]	QR-BLYP[a]	ECP-B3LYP[b]	Exp.[c]
ν_1 (a_{1g})	654	653	667 (672)	642	587	650	634	632	628
ν_2 (e_g)	541	552	534 (540)	539	529	530	535	547	523
ν_3 (t_{2u})	618	647	626 (634)	614	625	624	610	644	616
ν_4 (t_{1u})	185	191	186 (186)	197	217	195	210	243	203
ν_5 (t_{2g})	183	178	200 (200)	194	212	205	207	248	211
ν_6 (t_{2u})	141	150	143 (143)	163	186	165	187	219	173
Average error	8.0	14		7.0	19		8.2	30	

[a] This work.
[b] Ref. 13.
[c] Gas phase; cited from ref. 13.
[d] Estimated experimental harmonic frequencies in parentheses.

tal harmonic frequencies have been estimated for UF_6. As noted in Table II, the effect of anharmonicity is seen to be small, at 5–8 cm^{-1} for stretching modes, and negligible for bending modes. Using the harmonic frequencies, we obtain average deviations of 9 cm^{-1} (QR-BLYP), 31 cm^{-1} (ECP-BLYP), and 13 cm^{-1} (ECP-B3LYP), respectively. We can conclude that the comparison of calculated harmonic frequencies to experimental values introduces only small errors.

A more detailed discussion of the hexafluorides has been given elsewhere.[13]

2. GEOMETRIES AND VIBRATIONAL FREQUENCIES OF URANYL COMPOUNDS $[UO_2X_4]^{2-}$ (X = F, Cl, OH)

$[UO_2(OH)_4]^{2-}$. Calculated[167] and experimental[168] bond lengths of uranyl tetrahydroxide (VI), $[UO_2(OH)_4]^{2-}$, have been collected in Table III. We

TABLE III.
Experimentally and Theoretically Determined Structure of $[UO_2(OH)_4]^{2-}$ Ion.

U=O bond distance (Å)	U—O(H) bond distance (Å)	Method
1.80 (1)	2.21 (1)	EXAFS solution measurement; highly basic aqueous solution[a]
1.801 (6), 1.829 (6) 1.835 (5) 1.823 (5)	2.270 (4), 2.261 (5) 2.262 (5), 2.229 (5) 2.249 (5), 2.275 (5)	X-ray structure of $[Co(NH_3)_6]_2[UO_2(OH)_4]_3 \cdot 2H_2O$[a,b]
1.842	2.334	ECP-B3LYP calculations, minimum energy structure (D_{2d})[c,d]
1.892	2.360	ECP-BLYP calculations, minimum energy structure (D_{2d})[d]
1.867	2.302	OR-BLYP calculations, minimum energy structure (D_{2d})[e]

[a] Ref. 168. The solution measurements also indicate the presence of species with higher coordination number than in $[UO_2(OH)_4]^{2-}$.
[b] The unit cell contains three distinct $[UO_2(OH)_4]^{2-}$ ions. The average values are 1.826 (7) Å and 2.260 Å for the uranyl and hydroxide bond lengths, respectively.
[c] Ref. 167.
[d] ECP calculations with the Gaussian-94 program.[96,176]
[e] QR calculations with the ADF program.[170–172,178–181]

recently studied this molecule in some detail using the ECP-B3LYP approach,[167] and we will discuss only few aspects at this point. For instance, we predicted the existence of several conformers that differ essentially only by their arrangement of the hydrogen atoms, and that are accordingly close in energy. However, only the minimum energy structure (D_{2d} symmetry) has been included in Table III. The optimized structure of this conformer is shown in Figure 2.

Experimental data have been obtained by both aqueous solution (EXAFS[207]) and by single-crystal X-ray diffraction.[168] The unit cell of the $[Co(NH_3)_6]_2[UO_2(OH)_4]_3 \cdot 2H_2O$ crystals contains three distinct $[UO_2(OH)_4]^{2-}$ ions (Table III). We speculated earlier that these three ions may correspond to more than one of the predicted gas-phase conformers.[167] Of the three calculated structures, we note that the uranyl and hydroxide bond lengths are calculated to be too long by all methods. The ECP-B3LYP result comes closest to both the solution and solid-state measurements for the uranyl bond length, whereas the QR-BLYP calculation gives the best prediction for the equatorial hydroxide bond length. For the experimental solution studies the EXAFS results[168] also indicate the presence of species with a higher coordination number than in $[UO_2(OH)_4]^{2-}$, and this aspect may cloud the comparisons with the solution data. The ECP-BLYP values are again clearly too long, by about 0.06 Å for the uranyl bond, and by almost 0.1 Å for the hydroxide ligands. It is well known[208–211] that the BLYP approximation overestimates bond lengths; this feature is reproduced here. The QR method gives shorter bond lengths than the ECP approach for the same functional. It is possible that this is, at least partly, a basis-set effect.

The trends in the geometries are again visible in the calculated vibrational frequencies. Calculated and experimental[168, 212, 213] uranyl stretching frequencies are shown in Table IV. The calculated ECP-BLYP value for the symmetric ν_1 mode is almost 130 cm^{-1} too low as compared with experiment, reflecting that the bond lengths were seriously overestimated. Both the ECP-B3LYP and QR-BLYP ν_1 frequencies are much closer to the experimental value; they are still somewhat low, again in accordance with the bond lengths.

$[UO_2Cl_4]^{2-}$. We have also studied systems in which the OH^- ligands of $[UO_2(OH)_4]^{2-}$ are replaced by other groups. An important example is the $[UO_2Cl_4]^{2-}$ system (Fig. 2). Its electronic structure has been studied earlier by Pershina et al.[199, 200] These authors used an assumed geometry, along with a rather simple electronic structure method, and hence did not calculate bond lengths or vibrational frequencies.

Numerous crystal structures have been published that contain the $[UO_2Cl_4]^{2-}$ ion.[214–223] Some representative examples are given in Table V, along with solution measurements.[224] The calculated bond distances have been included as well. The uranyl bond lengths as obtained by X-ray vary considerably, as do the U—Cl distances (Table V). The ranges covered are 1.72–1.81 Å for the U=O bond lengths, and 2.62–2.71 Å for the chloride distances.[214] Such large variations in the solid state make an evaluation of the theoretical methods (that model a gas-phase molecule) rather difficult. Nevertheless, we note that the ECP-BLYP bond distances are overestimated; the other two methods give numbers that either fall into the experimental range (U=O distance), or are at least much closer to it (U—Cl distance). By comparing with

TABLE IV.
Calculated and Experimental Symmetric (ν_1, Raman Active) and Asymmetric (ν_2, IR Active) Uranyl Stretching Frequencies in $[UO_2X_4]^{2-}$ Ions (cm^{-1}).

Molecule	Freq.	QR-BLYP	ECP-BLYP	ECP-B3LYP	Experiment
$[UO_2(OH)_4]^{2-}$	ν_1	742	658	739[a]	784, 786[b]
	ν_2	804	751	823[a]	
$[UO_2Cl_4]^{2-}$	ν_1	818	740	835	836,[c] 833,[c] 854[d]
	ν_2	901	836	919	918,[c] 919[c]
$[UO_2F_4]^{2-}$	ν_1	766	682	771	822[d]
	ν_2	825	766	844	

[a]Ref. 167.
[b]Ref. 168.
[c]Ref. 212.
[d]Ref. 213.

the EXAFS[207] solution measurements,[224] we note that all theoretical methods overestimate the bond distances. The experimental uranyl bond length is again best predicted by the ECP-B3LYP method, with a deviation of only 0.02 Å or less. The equatorial chloride bond length is reproduced most closely by QR-BLYP. Note that these trends are very similar to the case of uranyl tetrahydroxide (VI); see earlier and Table III.

More conclusive answers regarding the theoretical geometries can perhaps be expected from the vibrational frequencies. We have seen previously that the calculated frequencies follow closely the trends in bond lengths. Hence, good agreement in the calculated frequencies for some particular structure may indicate that this geometry is close to the experimental conditions. Calculated and experimental[212–214, 225, 226] vibrational frequencies have been collected in Table VI. Starting with the three uranyl modes, the two uranyl stretching frequencies and the uranyl bending frequency, we note that they are best reproduced by the ECP-B3LYP approach, where we observe excellent

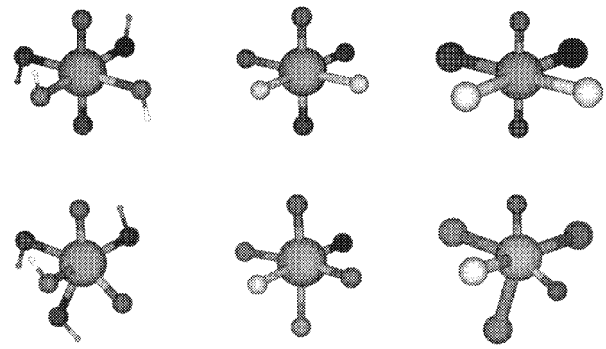

FIGURE 2. Minimum energy ''trans-uranyl'' (upper row) as well as ''cis-uranyl'' structures (lower row) of the uranyl (VI) compounds $[UO_2X_4]^{2-}$, X = OH, F, Cl. The structures shown here have been optimized at the ECP-B3LYP level of theory (see text).

TABLE V.
Calculated (''Trans-Uranyl'' Conformer) and Selected Experimental (X-Ray Diffraction and EXAFS) Structures of the $[UO_2Cl_4]^{2-}$ Ion.

U=O bond distance (Å)	U—Cl bond distance (Å)	Compound / method	
1.780	2.784	ECP-B3LYP calculations[a]	
1.826	2.811	ECP-BLYP calculations[a]	
1.799	2.730	QR-BLYP calculations[b]	
1.724 (7)	2.646 (4), 2.660 (3)	$[N(CH_3)_4][UO_2Cl_4]$[c, d]	(X-ray)
1.751 (9)	2.644 (3), 2.650 (4)	$Rb_2[UO_2Cl_4] \cdot 2H_2O$[e]	(X-ray)
1.76 (1)	2.676 (4), 2.692 (6)	$[Ca(OH_2)_3$(15-*crown*-5)$][UO_2Cl_4]$[f]	(X-ray)
	2.630 (5), 2.675 (5)		
1.763 (3)	2.657 (1), 2.706 (1)	$[(H_5O_2)_2$(18-*crown*-6)$][UO_2Cl_4]$[g]	(X-ray)
1.770 (3)	2.692 (2), 2.657 (2)	$[C_3N_2H_5]_2[UO_2Cl_4]$[h]	(X-ray)
1.784 (2)	2.705 (6), 2.697 (6)	$[LH]_2[UO_2Cl_4] \cdot 2H_2O$[c, i]	(X-ray)
1.789 (12)	2.706 (4), 2.699 (6)		
1.81	2.62	$Cs_2[UO_2Cl_4]$[c, j]	(X-ray)
1.760 (6)	2.67 (1)	aqueous solution (EXAFS)[k]	

[a] ECP calculations with the Gaussian-94 program.[96, 176]
[b] QR calculations with the ADF program.[170–172, 178–181]
[c] Ref. 214.
[d] Ref. 215.
[e] Ref. 223.
[f] Ref. 219.
[g] Ref. 221.
[h] Ref. 216.
[i] L = 2,6-diacetylpyridine-bisphenyl hydrazone.[214]
[j] Ref. 220; the experimental uncertainty is not given.
[k] Ref. 224; aqueous solution.

agreement between theory and experiment. The agreement with the experimentally observed frequencies is poorer for the other two methods, although QR-BLYP is still fair. The equatorial Cl modes are best represented by the QR-BLYP method, followed closely by the ECP-B3LYP results (Table VI). The agreement between theory and experiment is worst for the two lowest modes, where we expect medium effects to be relatively more important than for the other experimental frequencies. The ECP-BLYP frequencies are again too small throughout, indicating that the calculated bond lengths are far too long. These trends in the calculated frequencies confirm our discussion of the calculated bond lengths, and hence give additional confidence in the experimental solution (EXAFS) measurements.[224]

$[UO_2F_4]^{2-}$. If there were too many different X-ray structures for the $[UO_2Cl_4]^{2-}$ ion, then the situation is simply reversed for the $[UO_2F_4]^{2-}$ system—there are no known crystal structures in the literature. Rather, uranyl fluoride systems crystallize as dimers,[227] as neutral UO_2F_2 with six equatorial fluorine ligands per uranium atom (this is uranyl fluoride proper[228,229]), as $[UO_2F_5]^{3-}$ ions,[230–232] with other equatorial ligands[233] (e.g., $[UO_2F_4(H_2O)]^{2-}$ [234] or $[UO_2F_4(H_2O)_2]^{2-}$ [235]) and so on. However, all possible $[UO_2F_n]^{2-n}$ species ($n = 0-5$) have been shown to exist in solution.[213,236,237] Anhydrous tetrafluorodioxouranates (VI), $A_2[UO_2F_4]$ (A = Na, K, NH_4), have also been synthesized,[235] although no crystal structure has been resolved. In addition, the uranium oxyfluoride species, UO_2F_2, UO_2F, and UOF_4, have been isolated in a solid argon matrix.[238]

We chose the system with n = 4 as a representative example because it fits into the series of $[UO_2X_4]^{2-}$ ions, and it also allows the study of different ligands and their influence on the existence and stability of ''cis-uranyl'' conformers (see next subsection). Calculated geometries are shown in Table VII. As could be expected from the other examples, the longest bond lengths are predicted by ECP-BLYP; the calculated U—F bond length is shortest for QR-BLYP, and the uranyl bond length is shortest for ECP-B3LYP. Experimental[227,233,234]

TABLE VI.
Calculated and Experimental Vibrational Frequencies of $[UO_2Cl_4]^{2-}$.

Mode (D_{2d})	Assignment (D_{2d} symmetry)[a]	Frequencies (cm^{-1}) QR-BLYP	ECP-BLYP	ECP-B3LYP	Experiment (solid)	Experiment (solution)
1E	Cl — U — Cl bending (IR)	75	68	73	96,[b] 112[c,d]	
$1A_1$	UCl_4 deformation (R)	75	68	70	125,[b] 112[c,d]	121[e]
$1B_1$	UCl_4 deformation (R)	95	83	92	131[c]	
$1B_2$	Cl — U — Cl bending (IR)	109	99	103	119[b]	
$2B_2$	UCl_4 asymmetric stretch (R)	192	171	184	232,[b] 230[f]	
2E	OUCl bending (R)	191	178	186	202[b]	207[e]
3E	UCl_4 asymmetric stretch (IR)	206	191	204	233,[b] 238[c]	238[e]
$2A_1$	UCl_4 symmetric stretch (R)	228	202	218	256,[b] 264[c]	258[e]
4E	UO_2 bending (IR)	239	236	263	259,[b] 252,[c] 235[g]	262[e]
$3A_1$	UO_2 symmetric stretch (R)	818	740	835	836,[b] 831,[f] 812,[g] 833[g]	833,[e] 854[h]
$3B_2$	UO_2 asymmetric stretch (IR)	901	836	919	918,[b] 916,[c] 913,[g] 910[g]	919[e]

[a] R and IR stand for Raman and IR active modes, respectively.
[b] Ref. 212; solid $[Bu_4N]_2[UO_2Cl_4]$.
[c] Ref. 225; solid $Cs_2[UO_2Cl_4]$.
[d] Only one IR absorption observed for these two modes.
[e] Ref. 212; CH_2Cl_2 solution.
[f] Ref. 214.
[g] Ref. 226; solid $[UO_2Cl_4](PyH)_2$ and $[UO_2Cl_4](Py_2H)_2$, respectively.
[h] Ref. 213; aqueous solution.

TABLE VII.
Calculated Structure of $[UO_2F_4]^{2-}$ Ion, "Trans-Uranyl" Conformer.

U=O bond distance (Å)	U—F bond distance (Å)	Method
1.823	2.259	ECP-B3LYP[a]
1.870	2.276	ECP-BLYP[a]
1.847	2.205	QR-BLYP[b]
1.762	2.207	HF-ECP[c]

[a] ECP calculations with the Gaussian-94 program.[96,176]
[b] QR calculations with the ADF program.[170–172,178–181]
[c] Hartree–Fock calculations by Pyykkö et al.,[158] using a different ECP [201] and basis sets.

structures of uranyl fluoride systems show uranyl bond lengths in the range 1.77–1.82 Å, so that it is likely that this parameter is again somewhat overestimated even by ECP-B3LYP.

Calculated and experimental[213] values for the Raman active ν_1 vibrational mode of $[UO_2F_4]^{2-}$ are shown in Table IV. All theoretical methods underestimate the value of this frequency. This indicates that, indeed, the calculated uranyl bond lengths are too long. All three theoretical methods reproduce the experimentally observed reduction in the symmetric uranyl stretching frequency in going from X = Cl to X = F and X = OH (Table IV).

3. "CIS-URANYL" CONFORMERS OF $[UO_2X_4]^{2-}$ (X = F, Cl, OH)

In our recent study[167] on $[UO_2(OH)_4]^{2-}$, we were able to characterize not only various structures with the usual linear uranyl bond, but, additionally, stable conformers with a bent uranyl bond ("cis-uranyl") (Fig. 2). These conformers that represent local minima on the potential energy surface were predicted[167] to be only 18–19 kcal/mol higher in energy than the global energy minimum (ECP-B3LYP), and the calculated uranyl bond angles cover a range of 113° to 132°. Such structures are experimentally not known but they appear to play a crucial role as stable intermediates in intramolecular oxygen ligand-exchange processes.[167,168] We intend to continue and extend the investigation of "cis-uranyl" structures with the present studies.

Energies and key geometry parameters for "cis-uranyl" conformers of the $[UO_2X_4]^{2-}$ ions (X = OH, F, Cl) are shown in Table VIII. We have calculated the vibrational frequencies for each of these structures. In this way, we confirmed that the "cis-uranyl" conformers represent local minima on their potential energy surfaces at each level of theory. The structural parameters for a given compound vary considerably among the three theoretical methods. The longest calculated bond lengths are consistently those of the ECP-BLYP approach, and we can assume that they are too

TABLE VIII.
Stable "Cis-Uranyl" Structures of the $[UO_2X_4]^{2-}$ Ions, X = F, Cl, OH.

Molecule	Method	Energy[a] (kcal / mol)	Uranyl bond lengths (Å)	U—X bond lengths (Å)	Uranyl bond angle (degrees)
$[UO_2(OH)_4]^{2-}$	ECP-B3LYP[b]	18.0[d]	1.874, 1.870[d]	2.267, 2,320 2.349, 2.349[d]	128.4[d]
	ECP-BLYP[b]	10.8	1.923, 1.918	2.301, 2.345 2.374, 2.374	125.9
	QR-BLYP[c]	15.3	1.926, 1.894	2.271, 2.237 2.299, 2.299	103.5
$[UO_2F_4]^{2-}$	ECP-B3LYP[b]	23.5	1.887	2.177, 2.266	99.2
	ECP-BLYP[b]	14.7	1.932	2.207, 2.290	99.2
	QR-BLYP[c]	13.7	1.895	2.168, 2.202	95.8
$[UO_2Cl_4]^{2-}$	ECP-B3LYP[b]	30.3	1.813	2.746, 2.818	121.8
	ECP-BLYP[b]	20.5	1.874	2.747, 2.839	107.1
	QR-BLYP[c]	20.7	1.843	2.702, 2.734	98.1

[a] Relative to the respective "trans" structure.
[b] ECP calculations with the Gaussian-94 program.[96,176]
[c] QR calculations with the ADF program.[170–172,178–181]
[d] Lowest energy structure of various possible "cis-uranyl" conformer.[167]

long, based on previous experience. Calculated U=O bond lengths are generally shorter for the ECP-B3LYP method than for QR-BLYP, whereas U—X bond lengths show the opposite trend. Again, this is completely consistent with the results for the ''trans-uranyl'' conformers; see earlier and Tables III, V, and VII. Furthermore, the QR-BLYP calculations give the smallest uranyl bond angles by far. The reason is not entirely clear at the moment but it should be noted that the potential energy surface is fairly flat with respect to this parameter, and large changes in the O—U—O bond angle result in comparatively small changes in the total energy.

The calculated total energies vary considerably as well (Table VIII). It is of interest to note that the two BLYP approaches give energies that are fairly close to each other for X = F and Cl, whereas the ECP-B3LYP calculations predict all the ''cis-uranyl'' conformers to be less stable by up to 10 kcal/mol. Apparently, the choice of XC functional is more important for the ''cis–trans'' energy than the calculated bond lengths or the specific relativistic method.

The two ECP-based methods predict the following order for the stability of the ''cis'' conformers of $[UO_2X_4]^{2-}$: OH > F > Cl with the *cis*-$[UO_2Cl_4]^{2-}$ being least stable. The latter result is confirmed by the QR-BLYP calculations, whereas the order of X = OH and X = Cl is exchanged in this method: F ≈ OH > Cl for QR-BLYP. The differences in the calculated ''cis–trans'' energies are somewhat disappointing. Further studies are clearly required to establish the reliability and accuracy of DFT-based approaches for energetics of actinide compounds. Such benchmarking studies should compare energetics from different DFT approaches to well-established experimental data.

From the calculated numbers, it appears that the ''cis–trans'' energy separation correlates with the strength of the uranyl bond: a weak uranyl bond destabilizes the ''trans'' conformer, and the relative energy of the ''cis'' isomer decreases (Table IX). The strength of the uranyl bond can be inferred[168] from the bond length and the respective stretching frequency (Table IX). Indeed, the OH^- ligand is a strong π donor, which leads to π competition between equatorial and axial ligands, as has been discussed elsewhere.[167] This π competition results in a weak uranyl bond, which is evident from the very long uranyl bond and the low stretching frequency.[168]

TABLE IX.
Comparison of Calculated $[UO_2X_4]^{2-}$ Properties (ECP-B3LYP).[a]

X	R(U=O) (Å)	Symmetric uranyl stretching frequency ν_1 (cm^{-1})	E(''cis'') — E(''trans'') (kcal / mol)
OH	1.842	739	18.0
F	1.823	771	23.5
Cl	1.780	835	30.3

[a]Weaker U=O bonds lower energy of ''cis'' form.

Conclusions

The uranyl bond is an example of a very stable entity.[31] In all experimentally characterized examples, it has the linear (''trans'') arrangement of the three atoms. We predicted, however, the existence of stable structures with a bent (''cis'') uranyl bond for all three $[UO_2X_4]^{2-}$ species studied. The relative stability of the ''cis'' isomer seems to depend on the strength of the ''trans'' uranyl bond, and a weaker ''trans'' bond makes the ''cis'' form more accessible. The different theoretical methods gave a fairly wide range of ''cis–trans'' energies. Further studies on actinide molecules will be necessary to establish the accuracy and reliability of different DFT schemes for the calculation of relative energies. Such studies would need, as their basis, accurate experimental data, preferably measured in the gas phase—this type of data is still rather rare. Despite these technical difficulties, we found that the ''cis-uranyl'' structures are only some 10–30 kcal/mol higher in energy than the respective global energy minimum. Hence, it might become possible to synthesize and isolate uranyl complexes with a ''cis'' arrangement of the uranyl oxygens. Bulky ligands, possibly with multidentate coordination, might help to achieve this synthetic goal.

We have studied the bond lengths and vibrational frequencies as they were calculated by different methods. The ECP-BLYP approach consistently overestimated bond lengths (and underestimated frequencies accordingly). It thus reproduced a well-known feature of this XC functional.[208–211] In contrast, the QR-BLYP method gave consistently shorter bond lengths that were generally in better agreement with experiment. In

principle, putting aside basis-set differences, numerical integration issues, etc., this contraction should reflect the different approaches to relativity. It is difficult at this stage, however, to decide which is preferable, because changing the density functional to B3LYP resulted in bond length contractions of similar magnitude. Interestingly, ECP-B3LYP performed best in predicting the axial uranyl bond lengths (and frequencies) in all three $[UO_2X_4]^{2-}$ species, whereas QR-BLYP gave more reliable equatorial U—X bond lengths. Finally, we note that the ECP-B3LYP approach consistently overestimated the equatorial bond lengths in the uranyl species, sometimes by quite significant amounts.

Outlook and Future Directions

In this article, we have discussed the application of density functional theory to actinide-containing molecules. We will conclude with a short discussion of areas in which we foresee rapid development within the next few years.

We have seen how the theoretical description of actinide chemistry has benefited from the general advancement in DFT-based methods, the development of accurate approximations for the XC functional in particular. Various aspects of the progress in DFT methodology have also been discussed elsewhere in this special issue. DFT is increasingly becoming one of the most widely used choices for actinide calculations, especially for the study of environmentally relevant actinide compounds.[198] This is largely due to its accuracy and efficiency. These developments will undoubtedly continue as new ECPs[13,70–72] and other stable relativistic methods,[46,47,56–68] first and second derivatives of such relativistic expressions, the capability to handle high angular momentum basis functions (f, g, and higher), new XC model functionals, massively parallel computer codes,[178,239,240] and linear scaling methods[241–244] become generally available. All the developments mentioned are destined to benefit the theoretical study of actinide chemistry. To single out just one aspect, we expect the newly proposed stable relativistic two-component methods like DFT-ZORA[63–66] or DFT-DK[56–62] to be particularly useful in this part of the periodic table. The novel four-component relativistic methods[46,47] will find their applications, in particular, in the area of benchmark calculations as well as in the study of excited states.

New areas will be explored for the application of DFT to f-block chemistry. One example is the study of magnetic properties including the NMR chemical shift. The DFT-based theoretical methods[107] have advanced enough to appear useful for actinide problems, as has been discussed earlier. The inclusion of solvation effects[245–248] will be another new area in theoretical actinide chemistry. Much of experimental chemistry in general, and of actinide chemistry in particular, is done in solution. For instance, almost any question related to the fate of actinide compounds in the environment will be related to aqueous solutions.[198] Recent calculations on Fe^{3+} complexes in solution[245,248] using sophisticated solvent models give excellent results for hydrolysis reactions, and preliminary results for actinide species are encouraging.[249]

Although we have outlined many of the advances that have occurred in this field in recent years, calculations on actinide compounds still remain one of the most challenging areas for computational chemistry. Even the ''simpler'' closed-shell molecules with formal $5f^0$ configurations present computational hurdles in terms of SCF convergence, the overall size of the system, and the role of relativistic and electron correlation effects. The situation becomes significantly more complex from a computational standpoint when one approaches open-shell systems with $5f^n$ configurations, or even more complicated situations when the open-shell orbitals can be located either on the metal or the ligand.[162] Achieving SCF convergence becomes more problematic when there are a number of low-lying f orbitals that can be occupied, resulting in numerous competing states that are close in energy. One strategy incorporated in the ADF codes involves averaging over nearly degenerate electronic levels, resulting in fractional occupancies for the open-shell orbitals. For $5f^n$ systems with $n \geq 2$ the use of a single reference configuration as a zero-order description of the ground state may not be valid, if a number of $5f^n$ configurations are needed to describe the true electronic ground state.[120,121]

Furthermore, it becomes questionable whether spin-orbit effects can be neglected in these cases. This raises the issue of the proper treatment of spin–orbit effects in a DFT framework—a problem that is not yet completely solved at either the conceptual or practical level, especially for $5f^n$ systems with $n \geq 2$.[66] Although DFT in its original construction has been developed as a ground-state approach,[4–6], the method has been successfully

applied to various low-lying excited states in cases where the symmetries of the orbitals involved enable one to obtain separate SCF solutions for these states. Alternative approaches use propagator- and time-dependent methods to compute excited-state spectra of molecules within a DFT framework.[250–256]

It appears that actinide compounds will continue to present a formidable challenge to theoretical calculations to density functional as well as Hartree–Fock-based methods, because relativistic effects, electron correlation effects, multiplet interactions from electron–electron interactions, and spin–orbit effects all play important roles in determining the electronic properties of these systems.

Acknowledgment

The authors are grateful to our colleague, D. W. Keogh, for inspiring discussions. Furthermore, we thank D. L. Clark, D. W. Keogh, M. Dolg, J. Li, B. Bursten, S. K. Wolff, and T. Ziegler for providing preprints prior to publication.

References

1. Pepper, M.; Bursten, B. E. Chem Rev 1991, 91, 719.
2. Relativistic Hartree–Fock orbitals $\Phi_{nl}(r)$ obtained with the Cowan–Griffin approach[3] were calculated for the $5f^3$, $5f^26d^1$, $5f^27s^1$, and $5f^27p^1$ states of Pu^{3+}. The radial probability densities corresponding to $r^2\pi_{nl}(r)$ are plotted in Figure 1.
3. Cowan, R. D.; Griffin, D. C. J Opt Soc Am 1976, 66, 1010.
4. Hohenberg, P.; Kohn, W. Phys Rev 1964, 136, B864.
5. Kohn, W.; Sham, L. J Phys Rev 1965, 140, A1133.
6. Parr, R. G.; Yang, W. Density-Functional Theory of Atoms and Molecules; Oxford University Press: New York, 1989.
7. Ziegler, T. Chem Rev 1991, 91, 651.
8. Ziegler, T. Can J Chem 1995, 73, 743.
9. Seminario, J. M.; Politzer, P. (Eds.) Modern Density Functional Theory: A Tool for Chemistry; Elsevier: Amsterdam, 1995.
10. Chong, D. P. (Ed.) Recent Advances in Density Functional Methods; World Scientific: Singapore, 1995.
11. Laird, B. B.; Ross, R. B.; Ziegler, T. (Eds.) Chemical Applications of Density Functional Theory (ACS Symposium Series 629); American Chemical Society: Washington, DC, 1996.
12. Baerends, E. J.; Gritsenko, O. V. J Phys Chem A 1997, 101, 5383.
13. Hay, P. J.; Martin, R. L. J Chem Phys 1998, 109, 3875.
14. Frenking, G.; Antes, I.; Böhme, M.; Dapprich, S.; Ehlers, A. W.; Jonas, V.; Neuhaus, A.; Otto, M.; Stegmann, R.; Veldkamp, A.; Vyboishchikov, S. F. In K. B. Lipkowitz, and D. B. Boyd (Eds.) Reviews in Computational Chemistry; Verlag Chemie: Weinheim, 1996; p. 63.
15. Cundari, T. R.; Benson, M. T.; Lutz, M. L.; Sommerer, S. O. In K. B. Lipkowitz, and D. B. Boyd (Eds.) Reviews in Computational Chemistry; Verlag Chemie: Weinheim, 1996; p. 145.
16. Snijders, J. G.; Baerends, E. J. Mol Phys 1978, 36, 1789.
17. Snijders, J. G.; Baerends, E. J.; Ros, P. Mol Phys 1979, 38, 1909.
18. Boerrigter, P. M. PhD thesis, Free University, Amsterdam, The Netherlands, 1987.
19. Ziegler, T.; Snijders, J. G.; Baerends, E. J. J Chem Phys 1981, 74, 1271.
20. Ziegler, T.; Tschinke, V.; Baerends, E. J.; Snijders, J. G.; Ravenek, W. J Phys Chem 1989, 93, 3050.
21. Pauli, W. Z Phys 1927, 43, 601.
22. Foldy, L.; Wouthuysen, S. A. Phys Rev 1950, 78, 29.
23. Moss, R. E. Advanced Molecular Quantum Mechanics; Chapman and Hall: London, 1973.
24. Sakurai, J. J. Advanced Quantum Mechanics; Addison-Wesley: Redwood City, CA, 1967.
25. Berestetskij, V. B.; Lifshitz, E. M.; Pitaevskij, E. M. Relativistic Quantum Mechanics; Pergamon: Oxford, 1971.
26. McWeeny, R. Methods of Molecular Quantum Mechanics, 2nd Ed.; Academic: London, 1989.
27. Cohen, R. E.; Taylor, B. N. Phys Today 1987, 40, 11.
28. Pyykkö, P. Chem Rev 1988, 88, 563.
29. Pyykkö, P. In S. Wilson (Ed.) The Effect of Relativity on Atoms, Molecules, and the Solid State; Plenum: New York, 1991; p. 1.
30. Hess, B. A. Ber Bunsenges Phys Chem 1997, 101, 1.
31. Denning, R. G. Struct Bonding (Berl) 1992, 79, 215.
32. Bursten, B. E.; Strittmatter, R. J. Angew Chem Int Ed Engl 1991, 30, 1069.
33. Dolg, M.; Fulde, P. Chem Eur J 1998, 4, 200.
34. Pershina, V. G. Chem Rev 1996, 96, 1977.
35. Almlöf, J.; Gropen, O. In K. B. Lipkowitz and D. B. Boyd (Eds.) Reviews in Computational Chemistry; Verlag Chemie: Weinheim, 1996; p. 203.
36. Kaltsoyannis, N. J Chem Soc Dalton Trans, 1997, 1.
37. Hess, B. A.; Marian, C. M.; Peyerimhoff, S. D. In D. R. Yarkony (Ed.) Modern Electronic Structure Theory, Part I; World Scientific: Singapore, 1995; p. 152.
38. Engel, E.; Dreizler, R. M. Topics Curr Chem 1996, 181, 1.
39. King, R. B. Inorg Chem 1992, 31, 1978.
40. Dolg, M. In P. R. v. Schleyer (Ed.) Encyclopedia of Computational Chemistry; Wiley: New York, 1998.
41. Balasubramanian, K. In K. A. Gschneider, L. Eyring, G. R. Choppin, and G. H. Lander (Eds.) Handbook of Chemistry and Physics of Rare Earths, Vol. 18; Elsevier: Amsterdam, 1994; p. 29.
42. Dolg, M.; Stoll, H. In K. A. Gschneider and L. Eyring (Eds.) Handbook of Chemistry and Physics of Rare Earths, Vol. 22; Elsevier: Amsterdam, 1996; p. 607.
43. Dirac, P. A. M. Proc R Soc Lond (Series A) 1928, 117, 610.
44. Dirac, P. A. M. Proc R Soc Lond (Series A) 1928, 118, 351.
45. Breit, G. Phys Rev A 1929, 34, 553.

46. Liu, W.; Hong, G.; Dai, D.; Li, L.; Dolg, M. Theor Chem Acc 1997, 96, 75.
47. Liu, W.; Dolg, M. Phys Rev A 1998, 57, 1721.
48. Rosen, A.; Ellis, D. E. Chem Phys Lett 1974, 27, 595.
49. Rosen, A.; Ellis, D. E. J Chem Phys 1975, 62, 3039.
50. Ellis, D. E.; Goodman, G. L. Int J Quantum Chem 1984, 25, 185.
51. Ellis, D. E. In A. J. Freeman and G. H. Lander (Eds.) Handbook of Chemistry and Rare Earths, Vol. 2; Elsevier: Amsterdam, 1985; p. 1.
52. Kutzelnigg, W. Z Phys D 1990, 15, 27.
53. Douglas, M.; Kroll, N. M. Ann Phys (NY) 1974, 82, 89.
54. Hess, B. A. Phys Rev A 1986, 33, 3742.
55. Jansen, G.; Hess, B. A. Phys Rev A 1989, 39, 6016.
56. Knappe, P.; Rösch, N. J Chem Phys 1990, 92, 1153.
57. Rösch, N.; Häberlen, O. D. J Chem Phys 1992, 96, 6322.
58. Häberlen, O. D.; Rösch, N. Chem Phys Lett 1992, 199, 491.
59. Nasluzow, V. A.; Rösch, N. Chem Phys 1996, 210, 413.
60. Samzow, R.; Hess, B. A.; Jansen, G. J Chem Phys, 1992, 96, 6320.
61. Rösch, N.; Häberlen, O. D. J Chem Phys 1992, 96, 6322.
62. Boettger, J. G. Int J Quantum Chem 1997, 65, 565.
63. van Lenthe, E.; Baerends, E. J.; Snijders, J. G. J Chem Phys 1993, 99, 4597.
64. van Leeuwen, R.; van Lenthe, E.; Baerends, E. J.; Snijders, J. G. J Chem Phys 1994, 101, 1271.
65. van Lenthe, E.; van Leeuwen, R.; Baerends, E. J. Int J Quantum Chem 1996, 57, 281.
66. van Lenthe, E.; Snijders, J. G.; Baerends, E. J. J Chem Phys 1996, 105, 6505.
67. Mayer, M.; Häberlen, O. D.; Rösch, N. Phys Rev A 1996, 54, 4775.
68. Dyall, K. G. J Chem Phys 1997, 106, 9618.
69. The method has already been applied to UO_2^{2+}, PaO_2^{+}, and ThO_2 at the *ab initio* level (K. G. Dyall, private communication, 1998).
70. Küchle, W.; Dolg, M.; Stoll, H.; Preuss, H. J Chem Phys 1994, 100, 7535.
71. Ermler, W. C.; Ross, R. B.; Christiansen, P. A. Int J Quantum Chem 1991, 40, 829.
72. Nash, C. S.; Bursten, B. E.; Ermler, W. C. J Chem Phys 1997, 106, 5133.
73. T. V. Russo, R. L. Martin, and P. J. Hay, J Phys Chem, 1995, 99, 17085.
74. van Wüllen, C. Int J Quantum Chem 1997, 58, 147.
75. Raghavachari, K.; Curtiss, L. A. In D. R. Yarkony (Ed.) Modern Electronic Structure Theory, Part II; World Scientific: Singapore, 1995; p. 991.
76. Raghavachari, K.; Anderson, J. B. J Phys Chem 1996, 100, 12960.
77. Bartlett, R. J. In D. R. Yarkony (Ed.) Modern Electronic Structure Theory, Part II; World Scientific: Singapore, 1995; p. 991.
78. Head-Gordon, M. J Phys Chem 1996, 100, 13213.
79. Vosko, S. H.; Wilk, L.; Nusair, M. Can J Phys 1980, 58, 1200.
80. Slater, J. C. Phys Rev 1951, 81, 385.
81. Becke, A. D. Phys Rev A 1988, 38, 3098.
82. Perdew, J. Phys Rev B 1986, 33, 8822.
83. Lee, C.; Yang, W.; Parr, R. G. Phys Rev B 1988, 37, 785.
84. Perdew, J.; Wang, Y. Phys Rev B 1992, 45, 13244.
85. Becke, A. D. J Chem Phys 1993, 98, 5648.
86. Becke, A. D. In D. R. Yarkony (Ed.) Modern Electronic Structure Theory, Part II; World Scientific: Singapore, 1995; p. 1022.
87. Becke, A. D. J Chem Phys 1997, 107, 8554.
88. Ramana, M. V.; Rajagopal, A. K. Phys Rev A 1981, 24, 1689.
89. Ramana, M. V.; Rajagopal, A. K. Adv Chem Phys 1983, 54, 231.
90. Engel, E.; Keller, S.; Dreizler, R. M. Phys Rev A 1996, 53, 1367.
91. Schlegel, H. B. In D. R. Yarkony (Ed.) Modern Electronic Structure Theory, Part I; World Scientific: Singapore, 1995; p. 459.
92. Schreckenbach, G.; Li, J.; Ziegler, T. Int J Quantum Chem 1995, 56, 477.
93. Schreckenbach, G. PhD thesis, University of Calgary, Calgary, Alberta, Canada, 1996.
94. Breidung, J.; Thiel, W.; Komornicki, A. Chem Phys Lett 1988, 153, 76.
95. Breidung, J.; Thiel, W.; Komornicki, A. Inorg Chem 1991, 30, 1067.
96. Russo, T. V.; Martin, R. L.; Hay, P. J.; Rappé, A. K. J Chem Phys 1995, 102, 9315.
97. Ciu, Q.; Musaev, D. G.; Svensson, M.; Morokuma, K. J Phys Chem 1996, 100, 10936.
98. Kaupp, M.; Malkin, V. G.; Malkina, O. L.; Salahub, D. R. J Am Chem Soc 1995, 117, 1851.
99. Kaupp, M.; Malkin, V. G.; Malkina, O. L.; Salahub, D. R. Chem Phys Lett 1995, 235, 382.
100. Malkin, V. G.; Malkina, O. L.; Salahub, D. R. Chem Phys Lett 1996, 261, 335.
101. Schreckenbach, G.; Ziegler, T. Int J Quantum Chem 1996, 60, 753.
102. Schreckenbach, G.; Ziegler, T. Int J Quantum Chem 1997, 61, 899.
103. Ruiz-Morales, Y.; Schreckenbach, G.; Ziegler, T. J Phys Chem A 1997, 101, 4121.
104. Wolff, S. K.; Ziegler, T. J Chem Phys 1998, 109, 895.
105. Wolff, S. K.; Ziegler, T.; van Lenthe, E.; Baerends, E. J. J Chem Phys (submitted).
106. Schreckenbach, G.; Wolff, S. K; Ziegler, T. In J. C. Facelli, and A. de Dios, Eds.; Modelling Chemical Shifts (ACS Symposium Series) American Chemical Society: Washington, DC, 1999 (submitted).
107. Schreckenbach, G.; Ziegler, T. Theor Chem Acc 1998, 99, 71.
108. Some examples of *ab initio*-based theoretical studies on actinide molecules include references 33, 109–133.
109. Di Bella, S.; Gulino, A.; Lanza, G.; Fragalà, I.; Marks, T. J. Organometallics 1993, 12, 3326.
110. Di Bella, S.; Gulino, A.; Lanza, G.; Fragalà, I.; Marks, T. J. J Phys Chem 1993, 97, 11673.
111. Di Bella, S.; Lanza, G.; Fragalà, I.; Marks, T. J. Organometallics 1996, 15, 205.

112. Malli, G. L.; Da Silva, A. B. F.; Ishikawa, Y. J Chem Phys 1993, 101, 6829.
113. Da Silva, A. B. F.; Malli, G. L.; Ishikawa, Y. Can J Chem 1993, 71, 1713.
114. Malli, G. L.; Da Silva, A. B. F.; Ishikawa, Y. J Chem Phys 1994, 101, 6829.
115. Malli, G. L. Can J Chem 1992, 70, 421.
116. Malli, G. L.; Styszynski, J. J Chem Phys 1994, 101, 10736.
117. Malli, G. L.; Styszynski, J. J Chem Phys 1996, 104, 1012.
118. de Jong, W. A.; Nieuwpoort, W. C. Int J Quantum Chem 1996, 58, 203.
119. Visscher, L.; Dyall, K. G. Atom Nucl Data Tables 1997, 67, 207.
120. Ortiz, J. V.; Hay, P. J.; Martin, R. L. J Am Chem Soc 1992, 114, 2736.
121. Hay, P. J.; Martin, R. L. J Alloys Compd 1994, 213/214, 196.
122. Craw, J. S.; Vincent, M. A.; Hillier, I. H.; Wallwork, A. L. J Chem Phys 1995, 99, 10181.
123. Pepper, M.; Bursten, B. E. J Am Chem Soc 1990, 112, 7803.
124. Dolg, M.; Fulde, P.; Stoll, H.; Preuss, H.; Chang, A.; Pitzer, R. M. Chem Phys 1995, 195, 71.
125. Liu, W.; Dolg, M.; Fulde, P. J Chem Phys 1997, 107, 3548.
126. Küchle, W.; Dolg, M.; Stoll, H. J Phys Chem A 1997, 101, 7128.
127. Liu, W.; Dolg, M.; Fulde, P. Inorg Chem 1998, 37, 1067.
128. Chang, A. H. H.; Ermler, W. C.; Pitzer, R. M. J Chem Phys 1991, 94, 5004.
129. Chang, A. H. H.; Zhao, K.; Ermler, W. C.; Pitzer, R. M. J Alloys Compd 1994, 213/214, 191.
130. Zhao, K.; Pitzer, R. M. J Phys Chem 1996, 100, 4798.
131. Guo, T.; Diener, M. D.; Chai, Y.; Alford, M. J.; Haufler, R. E.; McClure, S. E.; Ohno, T.; Weaver, J. E.; Scuseria, G. E.; Smalley, R. E. Science 1992, 257, 1661.
132. Cornehl, H. H.; Heinemann, C.; Marcalo, A.; Pires de Matos, A.; Schwarz, H. Angew Chem Int Ed Engl 1996, 35, 891.
133. Hutschka, F.; Dedieu, A.; Troxler, L.; Wipff, G. J Phys Chem A 1998, 102, 3773.
134. Vanquickenborne, L. G.; Renders, A.; Pierloot, K.; Devoghel, D.; Görller-Walrand, C. Eur J Solid State Inorg Chem 1991, 28, 209.
135. Gulino, A.; Ciliberto, E.; Di Bella, S.; Fragalà, I.; Seyam, A. M.; Marks, T. J. Organometallics 1992, 11, 3248.
136. Gulino, A.; Di Bella, S.; Fragalà, I.; Casarin, M.; Seyam, A. M.; Marks, T. J. Inorg Chem 1993, 32, 3873.
137. Ciliberto, E.; Di Bella, S.; Gulino, A.; Fragalà, I.; Petersen, J. L.; Marks, T. J. Organometallics 1993, 11, 1727.
138. Bowmaker, G. A.; Görling, A.; Häberlen, O.; Rösch, N.; Goodman, G. L.; Ellis, D. E. Inorg Chem 1992, 31, 577.
139. Nash, C. S.; Bursten, B. E. New J Chem 1995, 19, 669.
140. Kaltsoyannis, N.; Bursten, B. E. Inorg Chem 1997, 34, 2735.
141. Kaltsoyannis, N.; Bursten, B. E. J Organomet Chem 1997, 528, 19.
142. Onoe, J.; Takeuchi, K.; Nakamatsu, H.; Mukoyama, T.; Sekine, R.; Kim, B. I.; Adachi, H. J Chem Phys 1993, 99, 6810.
143. Onoe, J.; Sekine, R.; Takeuchi, K.; Nakamatsu, N.; Mukoyama, T.; Adachi, H. Chem Phys Lett 1994, 217, 61.
144. Onoe, J. J Phys Soc Jpn 1997, 66, 2328.
145. Onoe, J.; Takeuchi, H.; Nakamatsu, H.; Mukoyama, T.; Sekine, R.; Adachi, H. Chem Phys Lett 1992, 196, 636.
146. Onoe, J.; Nakamatsu, H.; Mukoyama, T.; Sekine, R.; Adachi, H.; Takeuchi, K. Inorg Chem 1997, 36, 1934.
147. Wood, J. H.; Boring, A. M. Phys Rev B 1978, 18, 2701.
148. Cayton, R. H.; Novogradac, K. J.; Bursten, B. E. Inorg Chem 1991, 30, 2265.
149. Strittmatter, R. J.; Bursten, B. E. J Am Chem Soc 1991, 113, 552.
150. van Wezenbeek, E. M.; Baerends, E. J.; Snijders, J. G. Theor Chim Acta 1991, 81, 139.
151. van Wezenbeek, E. M. PhD thesis, Free University, Amsterdam, The Netherlands, 1992.
152. Haaland, A.; Martinsen, K.-G.; Swang, O.; Volden, H. V.; Booij, A. S.; Konings, R. J. M. J Chem Soc Dalton Trans 1995, 185.
153. Souter, P. F.; Kushto, G. P.; Andrews, L.; Neurock, M. J Am Chem Soc 1997, 119, 1682.
154. Kushto, G. P.; Souter, P. F.; Andrews, L. J Chem Phys 1997, 106, 5894.
155. Souter, P. F.; Kushto, G. P.; Andrews, L.; Neurock, M. J Phys Chem A 1997, 191, 1287.
156. Kushto, G. P.; Souter, P. F.; Andrews, L. J Chem Phys 1998, 108, 7121.
157. Heinemann, C.; Schwarz, H. Chem Eur J 1995, 1, 7.
158. Pyykkö, P.; Li, J.; Runeberg, N. J Phys Chem 1994, 98, 4809.
159. Kaltsoyannis, N. J Alloys Compd 1998, 271, 859.
160. Kaltsoyannis, N.; Scott, P. Chem Commun 1998, 1665.
161. Roussel, P.; Scott, P. J Am Chem Soc 1998, 120, 1070.
162. Li, J.; Bursten, B. E. J Am Chem Soc 1997, 119, 9021.
163. Arliguie, T.; Lance, M.; Nierlich, M.; Vigner, J.; Ephritikine, M. J Chem Soc Chem Commun 1995, 183.
164. Li, J.; Bursten, B. E. Preprint, 1998.
165. Li, J.; Bursten, B. E. J Am Chem Soc 1998, 120 (in press).
166. Li, J.; Bursten, B. E. Preprint, 1998.
167. Schreckenbach, G.; Hay, P. J.; Martin, R. L. Inorg Chem 1998, 37, 4442.
168. Clark, D. L.; Conradson, S. D.; Donohoe, R. J.; Keogh, D. W.; Morris, D. E.; Palmer, P. D.; Rogers, P. D.; Tait, C. D. Inorg Chem (in press).
169. Faradzel, A.; Smith, V. H., Jr. Int J Quantum Chem 1986, 29, 311.
170. Baerends, E. J.; Ellis, D. E.; Ros, P. Chem Phys 1973, 2, 41.
171. Baerends, E. J.; Ros, P. Chem Phys 1973, 2, 52.
172. Baerends, E. J. PhD thesis, Free University, Amsterdam, The Netherlands, 1973.
173. van Lenthe, E. PhD thesis, Free University, Amsterdam, The Netherlands, 1996.
174. Rohlfing, C. M.; Hay, P. J. J Chem Phys 1985, 83, 4641.
175. Li, J.; Schreckenbach, G.; Ziegler, T. J Am Chem Soc 1995, 117, 486.
176. Frisch, M. J.; Trucks, G. W.; Schlegel, H. B.; Gill, P. M. W.; Johnson, G.; Robb, M. A.; Cheeseman, J. R.; Keith, T.; Petersson, G. A.; Montgomery, J. A.; Raghavachari, K.; Al-Laham, M. A.; Zakrzewski, V. G.; Ortiz, J. V.; Foresman, J. B.; Cioslowski, J.; Stefanov, B. B.; Nanayakkara, A.;

Challacombe, M.; Peng, C. Y.; Ayala, P. Y.; Chen, W.; Wong, M. W.; Andres, J. L.; Replogle, E. S.; Gomperts, R.; Martin, R. L.; Fox, D. J.; Binkley, J. S.; Defrees, D. J.; Baker, J.; Stewart, J. P.; Head-Gordon, M.; Gonzalez, C.; Pople, J. A. Gaussian-94, Revision E.1; Gaussian: Pittsburgh, PA, 1995.

177. Hehre, W. J.; Radom, L.; von Schleyer, P. R.; Pople, J. A. Ab Initio Molecular Orbital Theory; Wiley: New York, 1986.
178. Fonseca Guerra, C.; Visser, O.; Snijders, J. G.; te Velde, G.; Baerends, E. J. In E. Clementi and C. Corongiu (Eds.) Methods and Techniques in Computational Chemistry METECC-95; Cagliari, 1995; p. 305.
179. ADF 2.3, Theoretical Chemistry, Vrije Universiteit, Amsterdam, 1997.
180. te Velde, G. Amsterdam Density Functional (ADF) User Guide, Release 2.3; Scientific Computing and Modelling, Chemistry Department, Vrije Universiteit, Amsterdam, The Netherlands, 1997.
181. te Velde, G.; Baerends, E. J. J Comp Phys 1992, 99, 84.
182. Boerrigter, P. M.; te Velde, G.; Baerends, E. J. Int J Quantum Chem 1988, 33, 87.
183. te Velde, G. PhD thesis, Free University, Amsterdam, The Netherlands, 1990.
184. Snijders, J. G.; Baerends, E. J.; Vernoijs, P. Atom Nucl Data Tables 1982, 26, 483.
185. Vernoijs, P.; Snijders, P. G.; Baerends, E. J. Slater Type Basis Functions for the Whole Periodic System [in Dutch], Internal Report; Department of Theoretical Chemistry, Free University, Amsterdam, 1981.
186. Krijn, J.; Baerends, E. J. Fit Functions in the HFS Method [in Dutch], Internal Report; Department of Theoretical Chemistry, Free University, Amsterdam, 1984.
187. Bérces, A.; Dickson, R. M.; Fan, L.; Jacobsen, H.; Swerhone, D.; Ziegler, T. Comput Phys Commun 1997, 100, 247.
188. Jacobsen, H.; Bérces, A.; Swerhone, D.; Ziegler, T. Comput Phys Commun 1997, 100, 263.
189. Fan, L.; Versluis, V.; Ziegler, T.; Baerends, E. J. Int J Quantum Chem Symp 1988, S22, 173.
190. Seip, H. M. Acta Chem Scand 1965, 20, 2698.
191. Weinstock, B.; Goodman, G. L. Adv Chem Phys 1965, 9, 169.
192. Hargittai, M. Coord Chem Rev 1988, 91, 35.
193. McDowell, R. S.; Asprey, L. B.; Paine, R. T. J Chem Phys 1974, 61, 3571.
194. Paine, R. T.; McDowell, R. S.; Asprey, L. B.; Jones, L. H. J Chem Phys 1976, 64, 3081.
195. Person, W. B.; Kim, K. C.; Campbell, M.; Dewey, H. J. J Chem Phys 1986, 85, 5524.
196. Dewey, H. J.; Barefield, E., II; Rice, W. W. J Chem Phys 1986, 84, 684.
197. Mulford, R. N.; Dewey, H. J.; Barefield, J. E., II. J Chem Phys 1991, 94, 4790.
198. Clark, D. L.; Hobart, D. E.; Neu, M. P. Chem Rev 1995, 95, 25.
199. Pershina, V. G.; Ionova, G. V.; Suraeva, N. I. Russian J Inorg Chem 1990, 35, 1178.
200. Ionova, G. V.; Pershina, V. G.; Suraeva, N. I. Russian J Inorg Chem 1991, 36, 175.
201. Hay, P. J.; Wadt, W. R.; Raffenetti, R. C.; Phillips, D. H. J Chem Phys 1979, 71, 1767.
202. Pulay, P.; Fogarasi, G.; Boggs, J. E. J Am Chem Soc 1979, 101, 2550.
203. Fogarasi, G.; Zhou, X. F.; Taylor, P. W.; Pulay, P. J Am Chem Soc 1992, 114, 8191.
204. Bérces, A.; Ziegler, T. J Phys Chem 1995, 99, 11417.
205. Bérces, A. J Phys Chem 1996, 100, 16538.
206. Bérces, A.; Ziegler, T. Topics Curr Chem 1996, 182, 41.
207. EXAFS is an acronym for extended X-ray absorption fine structure spectroscopy.
208. Johnson, B. G.; Gill, P. M. W.; Pople, J. A. J Chem Phys 1993, 98, 5612.
209. Russo, T. V.; Martin, R. L.; Hay, P. J. J Chem Phys 1995, 102, 8023.
210. Baker, J.; Muir, M.; Andzelm, J. W.; Scheiner, A. C. In B. B. Laird, R. B. Ross, and T. Ziegler (Eds.) Chemical Applications of Density Functional Theory (ACS Symposium Series 629); American Chemical Society, Washington, DC, 1996; p. 342.
211. Scheiner, A. C.; Baker, J.; Andzelm, J. W. J Comput Chem 1997, 18, 775.
212. Gál, M.; Goggin, P. L.; Mink, J. Spectrotchim Acta 1992, 48A, 121.
213. Nguyen-Trung, C.; Begun, G. M.; Palmer, D. A. Inorg Chem 1992, 31, 5280.
214. Keim, R.; Keller, C. (Eds.) Gmelin Handbook of Inorganic Chemistry (Supplement Volume C9); Springer: Berlin, 1979.
215. Di Sipio, L.; Tondello, E.; Pelizzi, G. Cryst Struct Commun 1974, 3, 297.
216. Perry, D.; Freyberg, D. P.; Zalkin, A. J Inorg Nucl Chem 1980, 42, 243.
217. Rogers, R. D.; Kurihara, L. K.; Benning, M. M. Inorg Chem 1987, 26, 4346.
218. Rogers, R. D. Acta Crystallogr 1988, C44, 638.
219. Rogers, R. D.; Bond, A. H.; Hipple, W. G. J Crystallogr Spectrosc Res 1990, 20, 611.
220. Hall, D.; Rae, A. D.; Waters, T. N. Acta Crystallogr 1974, 20, 160.
221. Rogers, R. D.; Bond, A. H.; Hipple, W. G.; Rollins, A. N.; Henry, R. F. Inorg Chem 1991, 30, 2671.
222. Brown, D. R.; Chippindale, A. M.; Denning, R. G. Acta Crystallogr 1996, C52, 1164.
223. Anson, C. E.; Al-Jowder, O.; Jayasooriya, U. A.; Powell, A. K. Acta Crystallogr 1996, C52, 279.
224. Allen, P. G.; Bucher, J. J.; Shuh, D. K.; Edelstein, N. M.; Reich, T. Inorg Chem 1997, 36, 4676.
225. Ohwada, K. Spectrochim Acta 1975, 31A, 973.
226. Kobets, L. V.; Khod'ko, M. N.; Kopashova, I. M.; Umreiko, D. S. Russian J Inorg Chem 1980, 25, 1314.
227. Ivanov, S. B.; Mikhailov, Y. N.; Kuznetsov, V. G.; Davidovich, R. l. J Struct Chem 1981, 22, 302.
228. Atoji, M.; McDermott, M. J. Acta Crystallogr 1970, B26, 1540.
229. Keller, C.; Keim, R. (Eds.) Gmelin Handbook of Inorganic Chemistry (Supplement Volume C8); Springer: Berlin, 1980.
230. Nguyen, Q. D. Bull Soc Chim Fr 1968, 3976.
231. Brusset, H.; Nguyen, Q. D. J Inorg Nucl Chem 1971, 33, 1365.

232. Garg, C. L.; Narasimham, K. V. Spectrochim Acta 1971, A27, 863.
233. Nguyen, Q. D.; Bkouche-Waksman, M.; Walewski, M.; Caceres, D. Bull Soc Chim Fr 1984, 129.
234. Mak, T. C. W.; Yip, W. H. Inorg Chim Acta 1985, 109, 131.
235. Bhattacharjee, M.; Chaudhuri, M. K.; Mandal, G. C.; Srinivas, P. J. Chem Soc Dalton Trans 1994, 2693.
236. Harada, M.; Fujii, Y.; Sakamaki, S.; Tomiyasu, H. Bull Chem Soc Jpn 1992, 65, 3022.
237. Szabó, Z.; Glaser, J.; Grenthe, I. Inorg Chem 1996, 35, 2036.
238. Souter, P. F.; Andrews, L. J Mol Struct (Theochem) 1997, 412, 161.
239. Guest, M. F.; Apra, E.; Bernholdt, D. E.; Fruchtl, H. A.; Harrison, R. J.; Kendall, R. A.; Kutteh, R. A.; Long, X; Nicholas, J. B.; Nichols, G. J. A.; Taylor, H. L.; Wong, A. T.; Fann, G. I.; Littlefield, G. J.; Nieplocha, J. Future Gen Comput Syst 1996, 12, 273.
240. Fruchtl, H. A.; Kendall, R. A.; Harrison, R. J.; Dyall, K. G. Int J Quantum Chem 1997, 64, 63.
241. Strain, M. C.; Scuseria, G. E.; Frisch, M. J. Science 1996, 271, 51.
242. White, C. A.; Johnson, B. G.; Gill, P. M. W.; Head-Gordon, M. Chem Phys Lett, 1996, 253, 268.
243. Challacombe, M.; Schwegler, E. J Chem Phys 1997, 106, 5526.
244. Schwegler, E.; Challacombe, M.; Head-Gordon, M. J Chem Phys 1997, 106, 9708.
245. Li, J.; Fisher, C. L.; Chen, J. L.; Bashford, D.; Noodleman, L. Inorg Chem 1996, 35, 4694.
246. Corcelli, S. A.; Kress, J. D.; Pratt, L. R.; Tawa, G. J. In L. Hunter and T. E. Klein (Eds.) Pacific Symposium on Biocomputing '96; World Scientific: Singapore, 1996; p. 142.
247. Pratt, L. R.; Tawa, G. J.; Hummer, G.; Garcia, A. E.; Corcelli, S. A. Int J Quantum Chem 1997, 64, 121.
248. Martin, R. L.; Hay, P. J.; Pratt, L. R. J Phys Chem A 1998, 102, 3565.
249. Martin, R. L.; Hay, P. J.; Schreckenbach, G.; Pratt, L. R. Unpublished results, 1998.
250. Bauernschmitt, R.; Ahlrichs, R. Chem Phys Lett 1996, 256, 454.
251. Gross, E. K. U.; Dobson, J. F.; Petersilka, M. Topics Curr Chem 1996, 181, 1.
252. Casida, M. E. In D. P. Chong (Ed.) Recent Advances in Density Functional Theory; World Scientific: Singapore, 1995; p. 155.
253. Jamorski, C.; Casida, M. E.; Salahub, D. R. J Chem Phys 1996, 104, 5134.
254. Casida, M. E.; Jamorski, C.; Bohr, F; Guan, J.; Salahub, D. R. In S. P. Karna and A. T. Yeates (Eds.) Nonlinear Optical Materials: Theory and Modeling (ACS Symposium Series 628); American Chemical Society: Washington, DC, 1996; p. 145.
255. Casida, M. E.; Jamorski, C.; Casida, K. C.; Salahub, D. R. J Chem Phys 1998, 108, 4439.
256. van Gisbergen, S. J. A.; Koostra, F.; Schipper, P. R. T.; Gritsenko, O. V.; Snijders, J. G.; Baerends, E. J. Phys Rev A 1998, 57, 2556.